Am J Physiol Lung Cell Mol Physiol 308: L931–L942, 2015.
First published February 6, 2015; doi:10.1152/ajplung.00107.2014.

Selective targeting of the α5-subunit of $GABA_A$ receptors relaxes airway smooth muscle and inhibits cellular calcium handling

George Gallos,[1] Gene T. Yocum,[1] Matthew E. Siviski,[1] Peter D. Yim,[1] Xiao Wen Fu,[1] Michael M. Poe,[2] James M. Cook,[2] Neil Harrison,[1] Jose Perez-Zoghbi,[3] and Charles W. Emala Sr.[1]

[1]*Department of Anesthesiology, College of Physicians and Surgeons of Columbia University, New York, New York;* [2]*Department of Chemistry, University of Wisconsin, Milwaukee, Wisconsin; and* [3]*Department of Cell Physiology and Molecular Biophysics; and Texas Tech University Health Sciences Center, Lubbock, Texas*

Submitted 22 April 2014; accepted in final form 5 February 2015

Gallos G, Yocum GT, Siviski ME, Yim PD, Fu XW, Poe MM, Cook JM, Harrison N, Perez-Zoghbi J, Emala CW Sr. Selective targeting of the α5-subunit of $GABA_A$ receptors relaxes airway smooth muscle and inhibits cellular calcium handling. *Am J Physiol Lung Cell Mol Physiol* 308: L931–L942, 2015. First published February 6, 2015; doi:10.1152/ajplung.00107.2014.—The clinical need for novel bronchodilators for the treatment of bronchoconstrictive diseases remains a major medical issue. Modulation of airway smooth muscle (ASM) chloride via $GABA_A$ receptor activation to achieve relaxation of precontracted ASM represents a potentially beneficial therapeutic option. Since human ASM $GABA_A$ receptors express only the α4- and α5-subunits, there is an opportunity to selectively target ASM $GABA_A$ receptors to improve drug efficacy and minimize side effects. Recently, a novel compound (*R*)-ethyl8-ethynyl-6-(2-fluorophenyl)-4-methyl-4*H*-benzo[*f*]imidazo[1,5-*a*][1,4] diazepine-3-carboxylate (SH-053-2′F-R-CH_3) with allosteric selectivity for α5-subunit containing $GABA_A$ receptors has become available. We questioned whether this novel $GABA_A$ α5-selective ligand relaxes ASM and affects intracellular calcium concentration ($[Ca^{2+}]_i$) regulation. Immunohistochemical staining localized the $GABA_A$ α5-subunit to human ASM. The selective $GABA_A$ α5 ligand SH-053-2′F-R-CH_3 relaxes precontracted intact ASM; increases GABA-activated chloride currents in human ASM cells in voltage-clamp electrophysiology studies; and attenuates bradykinin-induced increases in $[Ca^{2+}]_i$, store-operated Ca^{2+} entry, and methacholine-induced Ca^{2+} oscillations in peripheral murine lung slices. In conclusion, selective subunit targeting of endogenous α5-subunit containing $GABA_A$ receptors on ASM may represent a novel therapeutic option to treat severe bronchospasm.

$GABA_A$ α5-subunit; SH-053-2′F-R-CH_3; airway relaxation

DESPITE A PRESSING CLINICAL need for novel bronchodilators in the treatment of asthma and other bronchoconstrictive diseases, only three drug classes are currently in clinical use as acute bronchodilators in the United States (methylxanthines, anticholinergics, and β-adrenoceptor agonists) (6). An emerging novel pathway to achieve bronchodilation involves modulating airway smooth muscle (ASM) chloride conductance via $GABA_A$ receptors to achieve relaxation of human precontracted ASM (15). Although there is legitimate concern that widespread activation of all $GABA_A$ receptors may lead to undesirable side effects (sedation, hypnosis, etc.), we have shown that human ASM cells express a limited repertoire of $GABA_A$ receptor subunits, with the α4- and α5-subunits the only α-subunits expressed, thereby allowing for potential selective pharmacological tissue specific receptor targeting to minimize side effects (18, 33). Inhaled delivery of these selective compounds may also serve to obviate concerns of systemic effects. Concern regarding nonselective $GABA_A$ receptor activation is not limited to the airway. $GABA_A$ receptor ligands active in the central nervous system (CNS) can have many effects including anxiolytic, sedative, hypnotic, amnesic, anticonvulsant, and muscle relaxant effects. This motivated a search for benzodiazepine (BDZ) ligands that discriminate among the α-subunits of $GABA_A$ receptors (41, 42).

A novel approach to achieve this goal was developed by Cook and coworkers in the 1980s (1, 25) that employed a pharmacophore/receptor model based on the binding affinity of rigid ligands to BDZ/$GABA_A$ receptor sites (8). From this series of receptor models for $\alpha_{1-6}\beta3\gamma2$ subtypes a robust pharmacophore for α5-subtype selective ligands emerged resulting in the synthesis of a novel α5β3γ2 partial agonist modulator: (*R*)-ethyl 8-ethynyl-6-(2-fluorophenyl)-4-methyl-4*H*-benzo[*f*]imidazo[1,5-*a*][1,4]diazepine-3-carboxylate (or SH-053-2′-F-R-CH_3) (10). Given that α4- and α5-subunit-containing $GABA_A$ receptors are known to be present on ASM cells, it was of interest to examine the effects of this α5 BDZ/GABAergic subtype-selective agonist on ASM function and cellular signaling.

To assess this we performed immunohistochemistry to ascertain whether $GABA_A$ α5-subunits colocalized with smooth muscle α-actin in ASM intact sections from human upper airways and then questioned whether targeted activation of the restricted α5-subunit containing $GABA_A$ receptors on ASM cells would also elicit electrophysiological changes in ASM cells consistent with $GABA_A$ activation and relaxation of ASM.

The activation of $GABA_A$ receptors on ASM has been shown to elicit Cl^- conductance and membrane potential changes (18); the impact of these changes on known mechanisms relating to modulation of ASM tone has not been fully investigated. Since changes in membrane potential are known to affect ASM Ca^{2+} handling (39) and cytosolic Cl^- concentration ($[Cl^-]$) has been implicated in attenuating sarcoplasmic Ca^{2+} flux (21, 23), we questioned whether activation of α5-subunit-containing $GABA_A$ receptors on ASM could modulate intracellular calcium concentration ($[Ca^{2+}]_i$) and mediate relaxation of intact ASM.

MATERIALS AND METHODS

Reagents

Indomethacin, *N*-vanillylnonanamide (capsaicin analog), pyrilamine, acetylcholine, bradykinin, and gabazine were obtained from Sigma (St. Louis, MO). Tetrodotoxin was obtained from Calbiochem (San Diego, CA). SH-053-2′F-R-CH_3 was synthesized at the Depart-

Address for reprint requests and other correspondence: G. Gallos, Dept. of Anesthesiology, College of Physicians and Surgeons, Columbia Univ., 622 W. 168th St.; P&S Box 46, New York, NY 10032 (e-mail: gg2125@cumc.columbia.edu).

ment of Chemistry and Biochemistry, University of Wisconsin, Milwaukee (42).

Immunohistochemistry of Human ASM for GABA$_A$ Receptor α5-Subunit Protein Expression

All human airway tissue protocols were reviewed by Columbia University Institutional board and were deemed not human subjects research under 45 CFR 46. Human tracheal tissue was obtained from discarded airway from healthy lung donors during transplantation surgery at Columbia University. The trachea and first generation bronchi of the airway were processed for immediate fixation in 4% paraformaldehyde (4°C overnight), then incubated in 30% sucrose in PBS at 4°C for an additional 24 h prior to processing for cryostat sectioning (6 μm). The sections were washed in PBS, incubated with 0.1% Triton X-100 for 10 min, blocked with 15% goat serum, and then incubated overnight at 4°C in primary antisera. The primary antibodies used were *1*) anti-GABA α5 (rabbit, polyclonal; Chemicon no. AB9678, 1:300 dilution in PBS), and *2*) anti-α-smooth muscle actin (mouse, monoclonal; Sigma-Aldrich, no. A2547, 1:10,000 dilution in PBS). The secondary antibodies consisted of FITC-conjugated goat anti-rabbit IgG (1:400 dilution) and Alexa Fluor 594 goat anti-mouse IgG (1:400 dilution; Invitrogen) incubated for 1 h. Nuclear staining was performed with mounting medium premixed with DAPI stain (Vector Laboratories, no. H-1500). Negative controls omitted all primary antibodies but included secondary staining and nuclear staining steps. All the immunofluorescence experiments were repeated on at least three independent samples. Samples were viewed under confocal microscopy (Nikon A1 Eclipse) and images were acquired with NIS software version 4.10.

Force Measurements in Human ASM Strips

Human ASM strips were dissected from trachea and mainstem bronchi and epithelium was removed under a dissecting microscope. Strips were suspended at 1.5 g resting tension in Krebs-Henseleit (KH) buffer as previously described (17). Trachea and bronchi were obtained from surgical discards from healthy donor lungs incidental to lung transplant surgery, and studies were deemed not human subjects research after review by Columbia University's Institutional Review Board. KH buffer contained (in mM) 118 NaCl, 5.6 KCl, 0.5 $CaCl_2$, 0.24 $MgSO_4$, 1.3 NaH_2PO_4, 25 $NaHCO_3$, and 5.6 glucose, pH 7.4. Indomethacin (10 μM) was added to the buffer to block endogenous release of prostanoids. Strips were allowed to equilibrate for 1 h with KH buffer exchanges every 15 min. Strips underwent contractile challenges with acetylcholine (100 nM–100 μM) for three cycles with extensive buffer exchanges and resetting of resting tension to 1.5 g between cycles. Tetrodotoxin (1 μM), pyrilamine (10 μM), and MK501 (10 μM) were then added to the buffer to eliminate potentially confounding effects of neural activation, histamine release, or leukotriene release from other cell types (neurons, mast cells) present in the ASM strip preparation during muscle force studies. ASM strips were then contracted with an EC_{50} concentration of acetylcholine, and, after establishment of a stable plateau of muscle force (typically ~30 min), 10 nM of isoproterenol was added with or without 50 μM SH-053-2′F-R-CH_3 or vehicle (0.2% ethanol). The magnitude of remaining muscle force was measured 15 min after the addition of isoproterenol ± SH-053-2′F-R-CH_3 and expressed as a percentage of the initial acetylcholine-induced force.

Force Measurements in Guinea Pig Tracheal Rings

All animal protocols were approved by the Columbia University Animal Care and Use Committee. Male Hartley guinea pigs (~400 g) were anesthetized with intraperitoneal pentobarbital (100 mg/kg). Trachea were removed and dissected under a dissecting microscope into closed rings comprised of two cartilaginous segments. Epithelium was removed by gentle abrasion of the tracheal lumen with cotton. This method has been confirmed by histology to completely remove the epithelial layer without damaging the underlying smooth muscle layer. Tissues were placed into cold KH buffer containing 10 μM indomethacin as above.

Closed GP tracheal rings were suspended in organ baths as previously described (46). Briefly, tissues were hung in a water-jacketed (37°C) 2-ml organ bath (Radnoti Glass Technology, Monrovia, CA) and attached to a Grass FT03 force transducer (Grass Telefactor, West Warwick, RI) coupled to a computer via BioPac hardware and Acqknowledge 7.3.3 software (Biopac Systems, Goleta, CA). KH buffer was continuously bubbled with 95% oxygen and 5% carbon dioxide and tissues were allowed to equilibrate at 1 g isotonic force for 1 h with fresh KH buffer changes every 15 min.

Following equilibration, the capsaicin analog *N*-vanillylnonanamide (10 μM final) was added to the organ baths to first activate and then deplete nonadrenergic, noncholinergic nerves. After *N*-vanillylnonanamide-induced force had returned to baseline (~50 min), the tracheal rings were washed and then subjected to two cycles of increasing cumulative concentrations of acetylcholine (0.1 μM to 0.1 mM) to determine the EC_{50} concentrations of acetylcholine required for each individual ring. To avoid bias between treatment groups, tissues were contracted by using acetylcholine at the individually calculated EC_{50} value for each tissue, and tissues with similar E_{max} values were randomly assigned to treatments within individual experiments. To remove confounding effects of other procontractile pathways, each bath received a complement of antagonists 20 min prior to subsequent contractile challenge. The antagonists included pyrilamine (10 μM; H_1 histamine receptor antagonist), and tetrodotoxin (1 μM; Na^+ channel blocker to obviate neuronal-mediated cholinergic or C-fiber effects).

Guinea pig (GP) tracheal rings were contracted with either 10 mM tetraethylammonium chloride (TEA) (a nonselective K^+ channel blocker that induces membrane depolarization, external Ca^{2+} entry and contraction), or 1 μM substance P (a ligand that activates the Gq-coupled neurokinin receptors). Preliminary studies determined that 100 μM SH-053-2′F-R-CH_3 induced an ~50% relaxation of a substance P-induced contraction in guinea pig tracheal rings. After contractions achieved a steady-state plateau of increased force (typically 30 min), 50 or 100 μM SH-053-2′F-R-CH_3 or vehicle (0.2%, 0.4% ethanol) was added and the maintenance of force was measured after 30 min and was expressed as a percent of the initial contractile agonist-induced force.

Human ASM Cell Culture

Human immortalized bronchial smooth muscle cell lines prepared as described (19) were grown to confluence in M199 media (GIBCO) containing 10% fetal bovine serum, 0.25 ng/ml epidermal growth factor, 1 ng/ml fibroblast growth factor, ITS supplement (1 mg/ml insulin, 0.55 mg/ml transferrin, 0.67 μg/ml sodium selenium), and antibiotics (100 units/ml penicillin G sodium, 100 μg/ml streptomycin sulfate, 0.25 μg/ml amphotericin B) in a humidified atmosphere of 5% CO_2/95% air at 37°C. Twenty-four hours prior to studies, cells were fed with fresh media.

Electrophysiology of Human ASM Cells

To investigate whether targeted activation of α5-subunit-containing GABA$_A$ receptors induces electrophysiological changes in human ASM cells, we measured the effect of SH-053-2′F-R-CH_3 on membrane currents. On the day of the assay, immortalized human ASM cells were released from collagen-coated plates with collagenase type IV (Sigma C5138, 500 units/ml), centrifuged at 300 *g*, resuspended in SmBM2 medium (Lonza), and transferred into collagen-treated glass bottom 1-cm Petri dishes. Cells were then incubated at 37°C in 5% CO_2 95% air for 3–4 h, allowing for reattachment of cells. Following generation of membrane seals (40–120 MΩ), whole cell configuration

was used for current recordings under voltage (holding potential −60 mV) conditions. To determine a current-voltage (*I*-V) relationship, voltage was stepped from −40 to 100 mV in 10 mV increments in the absence and presence of SH-053-2′F-R-CH$_3$. Studies were performed with a 2-kHz Bessel filter, recording at 10 kHz with use of an Axopatch 200b amplifier (Axon Instruments, Foster City, CA). Perfusion for drug additions were made with the ALA VM-8, 8-chamber pressure-driven drug application system. Electrodes were pulled with a P-97 micropipette puller from 1.5-mm OD borosilicate capillary glass (Sutter Instruments, Novato, CA). All recordings were analyzed on Clampfit 8.0 software (Molecular Devices). Extracellular solutions contained (in mM) 130 CsCl, 10 HEPES (pH 7.4), 1 $MgCl_2$, 1.8 $CaCl_2$, and 10 glucose. Intracellular solutions contained (in mM) 130 CsCl, 5 MgATP, 5 EGTA, 1 $MgCl_2$, 5 $CaCl_2$, and 10 HEPES (pH 7.2).

To determine whether SH-053-2′F-R-CH$_3$ evoked-currents are GABA$_A$ receptor specific and do not represent "leak" currents, we also performed additional electrophysiology studies utilizing Nanion's Port-a-Patch chip technology (Nanion). Immortalized human ASM cells were released from collagen-coated plates with collagenase type IV (Sigma C5138, 500 units/ml) and centrifuged at 100 *g* for 2 min. The cell pellet was washed and reconstituted in extracellular recording solution (containing, in mM, 145 NaCl, 5 KCl, 1 $MgCl_2$, 1.8 $CaCl_2$, 10 TES, pH 7.3, 297 mosM) at a density of 1×10^6 cells/ml. Cells were added (5 μl) to the recording chamber of a 3–5 MΩ chip and screened for membrane seals above 450 MΩ (prior to establishing whole-cell configuration) and a subsequent baseline holding current of less than 2 nA (after establishing whole cell configuration). Cells that met these criteria were first tested for responsiveness to GABA (1 mM) and gabazine (500 μM). After confirmation of appropriate currents in the batch of dissociated cells, additional cells that met the above criteria underwent voltage-clamp recordings ($V_H = -60$ mV) of current evoked by the sequential addition of GABA (1 μM) followed by addition of vehicle (0.1% DMSO) or SH-053-2′F-R-CH$_3$ (100 μM) and a later addition of gabazine (500 μM). All drugs were prepared in the extracellular recording solution. The internal recording solution contained (in mM) 50 CsCl, 10 NaCl, 60 CsF, 20 EGTA, 10 mM TES, pH 7.3, 284 mosM. All patch-clamp recordings were performed at room temperature (20–24°C). Currents were recorded on an Axopatch 200B amplifier, filtered at 2 kHz, and analyzed with pClamp 10.2 software. Evoked currents were normalized to baseline currents for interexperimental analysis. The data represent recordings from cells isolated on 6 separate days.

Effect of SH-053-2′F-R-CH$_3$ on Agonist-Mediated Increases in Intracellular Calcium

To assess the functional impact of SH-053-2′F-R-CH$_3$ on receptor-Gq coupled Ca^{2+} handling, Fluo-4 AM assays were performed in immortalized human ASM cells. Three types of Ca^{2+} assays were performed after pretreatment of cells with SH-053-2′F-R-CH$_3$: *1*) the effect on bradykinin-induced increases on $[Ca^{2+}]_i$ (bradykinin is a ligand for one of several Gq-coupled receptors in ASM); *2*) the effect on bradykinin-induced increases in $[Ca^{2+}]_i$ when Ca^{2+} was omitted from the external buffer solution; and *3*) the effect on store-operated calcium entry (SOCE). Cells were grown to full confluence in black-walled, clear-bottomed 96-well plates. Medium bathing the cells was removed and the cells were washed with 100 μl (per well) of Hanks' balanced salt solution (HBSS) and then loaded with a solution (100 μl/well) containing 0.05% Pluronic F-127, 2.5 mM probenecid, and 5 μM Fluo-4 AM, dissolved in HBSS. The cells were then incubated for 30 min at 37°C with Fluo-4 AM, washed once, and incubated for an additional 30 min at 37°C (95% air, 5% CO_2) with HBSS containing 2.5 mM probenecid. Cells were then pretreated for 15 min with 10 μM SH-053-2′F-R-CH$_3$, 200 μM gabazine, or vehicle (0.1% DMSO) before the addition of 1 μM bradykinin by use of the automatic injection feature of the FlexStation 3 microplate reader (Molecular Devices, Sunnyvale, CA) during continuous fluorescent measurements. The cells were excited at 488 nm every 5 s, and emission data were continuously collected at 516 nm. Real-time changes in intracellular Ca^{2+} are reported as RFU (relative fluorescence units). Readings from at least three wells per treatment were collected and averaged for each *n* value.

Effect of SH-053-2′F-R-CH$_3$ on Store-Operated Calcium Entry

To determine the effect of SH-053-2′F-R-CH$_3$ on ASM SOCE, cells were loaded with Fura-2 AM calcium indicator (2.5 μM; 100 μl per well; Molecular Probes, Eugene, OR) for 45 min in HBSS. Following loading, the cells were washed and incubated at 37°C in Ca^{2+}-free HBSS with drug pretreatments for 15 min (100 μM SH-053-2′F-R-CH$_3$; 100 μM gabazine; SH-053-2′F-R-CH$_3$ plus gabazine; 10 μM SKF 96365; or 0.2% ethanol vehicle). To passively deplete the sarcoplasmic reticulum (SR) of Ca^{2+}, the cells were then treated with the sarco/endoplasmic reticulum Ca^{2+}-ATPase (SERCA) inhibitor thapsigargin (1 μM) for 11 min prior to reintroduction of external Ca^{2+} (2.5 mM). Fura-2 AM fluorescent signal (excitation 340/380 nm and emission 510 nm) was measured continuously by use of a Flex Station 3 plate reader (Molecular Devices, Sunnyvale, CA). Peak signal following Ca^{2+} reintroduction was normalized to the thapsigargin-induced response and presented as fraction of vehicle, as reported previously (44).

Effect of SH-053-2′F-R-CH$_3$ on Methacholine-Mediated Contraction and Calcium Oscillations Measured in Peripheral Murine Lung Slices

Preparation of lung slices. These studies were reviewed and approved by the Institutional Animal Care and Use Committee of the Texas Tech University Health Sciences Center (IACUC protocol no. 07069). Mouse lung slices were prepared as previously described (5, 34). Briefly, male C3H mice (8–12 wk) were killed with pentobarbital (40 mg/kg ip) and the chest cavity was opened to allow for cannulation of the trachea. The lungs were inflated with 1.4 ml of 2% agarose in HBSS, followed by ~0.2 ml of air. The agarose was gelled by cooling the lungs with a cotton ball soaked in ice-cold HBSS and maintaining the mouse body at 4°C for 20 min; following removal, the lungs and heart were held in ice-cold HBSS for 15 min. Lung lobes were transferred to the specimen syringe tube of a tissue slicer (Compresstome VF-300; Precisionary Instruments). The lung lobe was embedded first into ~1 ml of 2% agarose and then fully covered with 6% gelatin, after which the block was cut into serial sections of 140 μm. Lung slices containing small terminal airways were incubated in low-glucose Dulbecco's modified Eagle's medium supplemented with 1× antibiotic solution containing L-glutamine, penicillin, and streptomycin (Invitrogen) at 37°C and 10% CO_2 in a cell culture incubator for up to 48 h. Lung slices containing airways with a lumen diameter of 100–300 μm, completely lined by active ciliated epithelial cells, and fully attached to the surrounding lung parenchyma were used for experiments.

Measurement of airway contraction and $[Ca^{2+}]_i$ in lung slices. Measurements of changes in small-airway cross-sectional lumen area (lumen area hereafter) and the fluorescent measurements of $[Ca^{2+}]_i$ in ASM cells were performed as previously described (34). Briefly, lung slices were mounted in a custom-made perfusion chamber and airways were visualized by use of a ×10 objective. Digital images (640 × 488 pixels) were recorded in time lapse (0.5 Hz) by use of a charge-coupled device camera (KP-M1A; Hitachi), frame grabber (Picolo; Euresys), and image-acquisition software (Video Savant; IO Industries). The lumen area was normalized to the area before stimulation. In some experiments lung slices were loaded with Oregon green 488 BAPTA-1 acetoxymethyl ester (Invitrogen) for the intracellular imaging of Ca^{2+} as previously described (34). Changes in fluorescence intensity were analyzed by selecting regions of interest

(ROI) ranging from 25 to 49 square pixels. Average fluorescence intensities of an ROI were obtained, frame-by-frame, by using a custom-written script designed to track the ROI within a smooth muscle cell (as it moves due to airway contraction/movement). Final fluorescence values were expressed as a fluorescence ratio (F/F_0) normalized to the initial fluorescence (F_0). All experiments were performed at room temperature.

Statistical Analysis

Each experimental procedure included internal controls. Where appropriate, we employed repeated measures in a one-way ANOVA using Bonferroni posttest comparisons. In cases where only two experimental groups were compared, a two-tailed Student's *t*-test was employed. Data are presented as means ± SE; $P < 0.05$ in all cases was considered significant.

RESULTS

The GABA$_A$ Receptor α5-Subunit Is Expressed in ASM from Human Trachea

ASM dissected from the posterior wall of human tracheas demonstrated extensive immunoreactivity for the GABA$_A$ receptor α5-subunit (Fig. 1, *A* and *C*) that colocalized with immunoreactivity for smooth muscle specific α-actin (Fig. 1, *B* and *C*). Nonspecific staining was not detected when the primary antibodies were omitted (Fig. 1*D*).

A Ligand for GABA$_A$ Receptors Containing the α5-Subunit Augments β-Adrenoceptor Agonist-Mediated Relaxation in Human ASM

We also determined the ability of a ligand directed against GABA$_A$ receptors containing the α5-subunit to augment β-adrenoceptor agonist-mediated relaxation of precontracted human ASM. This is highly clinically relevant since acute rescue of precontracted ASM during an asthmatic exacerbation is accomplished with β-adrenoceptor agonists and cases of asthma refractory to standard β-adrenoceptor therapy are not uncommon (36). The ability of 10 nM isoproterenol to relax a precontracted strip of human ASM (acetylcholine EC_{50}) was significantly enhanced in the presence of SH-053-2′F-R-CH$_3$ (50 μM) compared with vehicle control (Fig. 2*A*), (n = 8/group $P < 0.01$).

A Ligand for GABA$_A$ Receptors Containing the α5-Subunit Directly Relaxes Depolarization- or Gq-Coupled-Induced Contractions in Guinea Pig ASM

In addition to augmenting β-agonist mediated relaxation, we questioned whether the GABA$_A$ α5 ligand SH-053-2′F-R-CH$_3$ could directly relax an established contraction induced by membrane depolarization with TEA as well as from activation of a receptor coupled to Gq. The maintenance of contractile force induced by TEA was directly and significantly relaxed by 50 μM SH-053-2′F-R-CH$_3$ compared with vehicle (Fig. 2, *B* and *C*) (n = 5/group, $P < 0.05$) and the maintenance of contractile force induced by substance P was directly and significantly relaxed by 100 μM SH-053-2′F-R-CH$_3$ compared with vehicle (Fig. 2, *D* and *E*) (n = 4–5/group, $P < 0.01$).

Whole Cell Electrophysiological Recordings of Human ASM Cells Demonstrate That the Selective Ligand for GABA$_A$ Receptors Containing α5-Subunits Induces a Cl$^-$ Current In Vitro

Having demonstrated functional relaxation of intact ASM from both human and guinea pig under three different contractile paradigms, we next investigated the cell signaling effects of SH-053-2′F-R-CH$_3$. Using the whole cell configuration we demonstrate a significant current in human ASM cells upon exposure to 10 μM SH-053-2′F-R-CH$_3$ (Δ−28 ± 7 pA current) compared with vehicle (Δ−6 ± 3 pA current; n = 4/group, $P < 0.05$) (Fig. 3, *A* and *B*). To confirm that these currents were indeed due to Cl$^-$ flux, we examined the *I*-V relationship in human ASM cells in the presence and absence of SH-053-2′F-R-CH$_3$ (10 μM) (representative tracing, Fig. 3*C*). For these studies, we used intracellular and extracellular solutions that were symmetrical for [Cl$^-$]. The predicted chloride equilibrium potential was 0.4 mV and the measured equilibrium potential was 0.73 mV. Additionally, we observed

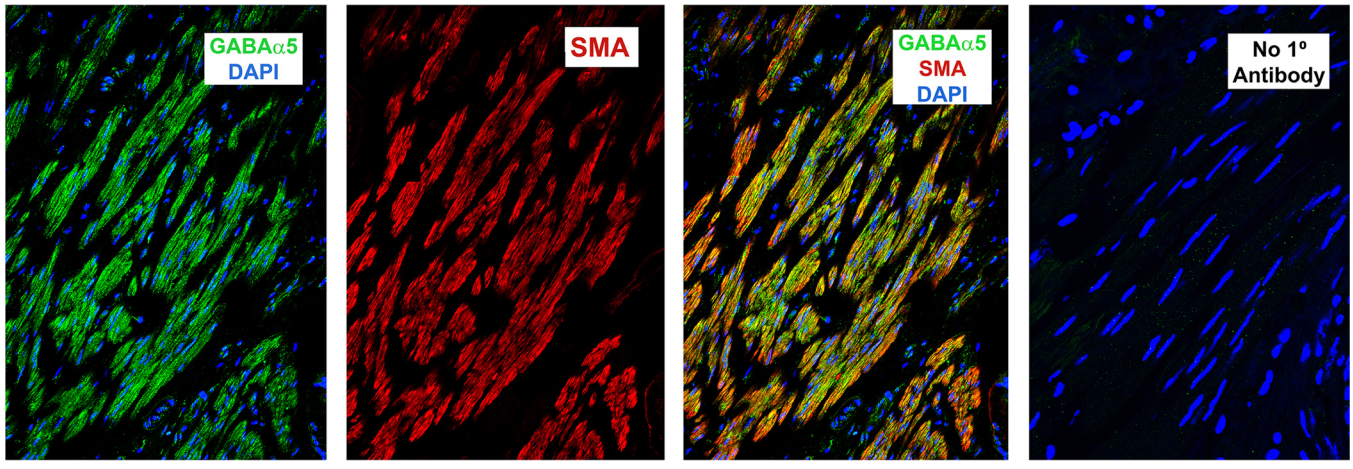

Fig. 1. Immunohistological characterization of the GABA$_A$ receptor α5-subunit protein expression in intact human tracheal airway smooth muscle (ASM). Confocal microscopy images employing single, double, and triple immunofluorescence labeling using antibodies directed against GABA$_A$ receptor α5 subunit (green), α-smooth muscle actin (SMA) (red), and/or the nuclear counterstain DAPI (blue). Representative images from native human tracheal ASM are depicted. DAPI and GABA$_A$ α5-subunit costaining, α-SMA alone, triple staining and merging of GABA$_A$ α5, α-SMA, and DAPI nucleus counterstain, with primary antibodies omitted as negative control.

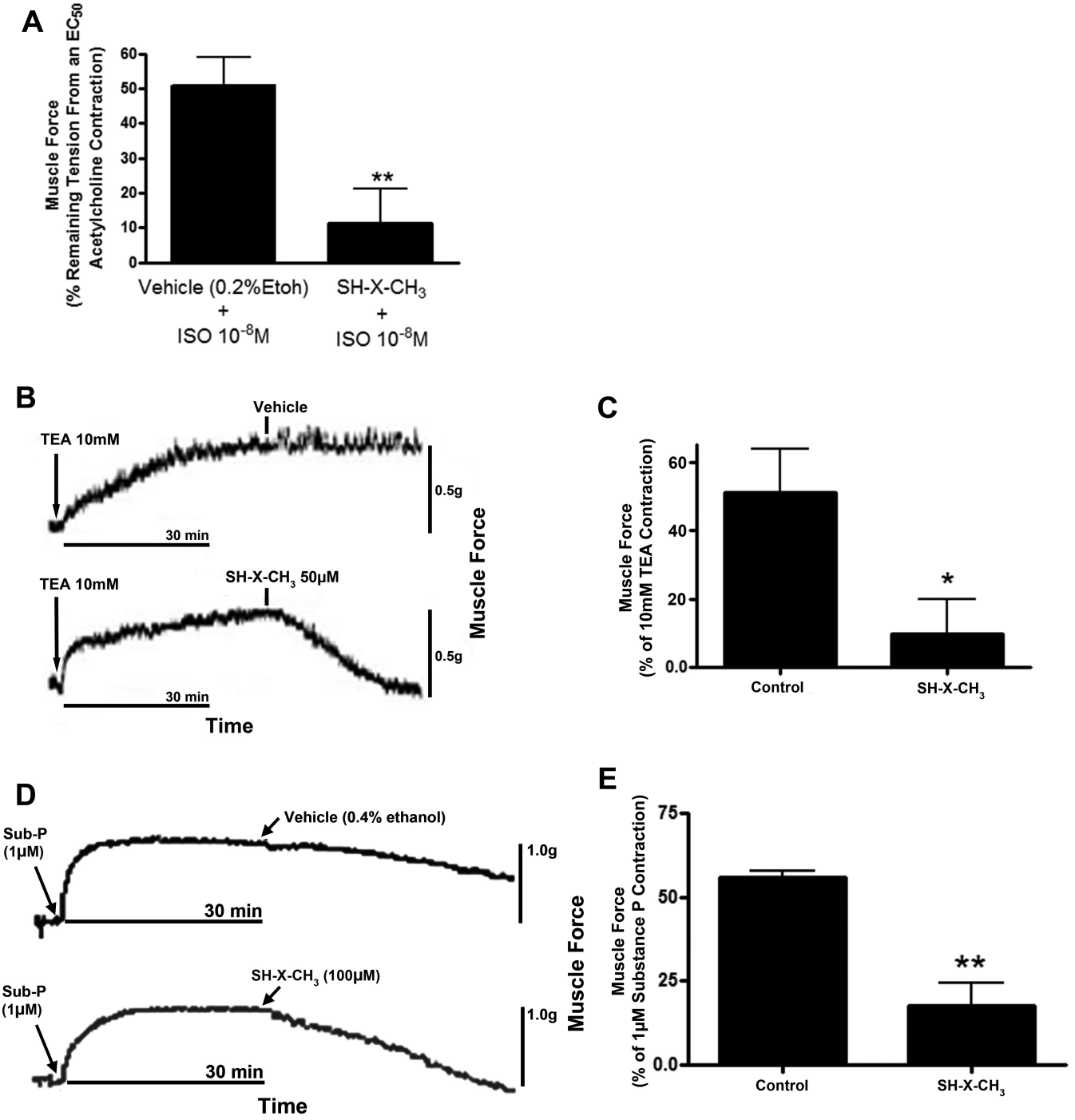

Fig. 2. Selective targeting of α5-subunit-containing GABA$_A$ receptors leads to functional relaxation of precontracted human and guinea pig ASM. *A*: the GABA$_A$ α5-subunit-targeting ligand SH-053-2′F-R-CH$_3$ potentiates β-adrenoceptor agonist-mediated relaxation of human ASM. Human ASM strips were contracted with an EC$_{50}$ concentration of acetylcholine and then treated with 10 nM isoproterenol (ISO) and 50 μM SH-053-2′F-R-CH$_3$ (SH-X-CH$_3$) or 10 nM isoproterenol and vehicle [0.2% ethanol (Etoh)]. The percent of remaining muscle force of the acetylcholine-induced contraction was measured at 15 min. SH-053-2′F-R-CH$_3$ significantly enhanced isoproterenol relaxation compared with its vehicle (n = 8/group, $^{**}P < 0.01$). *B* and *C*: the GABA$_A$ α5-subunit-targeting ligand SH-053-2′F-R-CH$_3$ relaxes an established contraction induced by a depolarization stimulus with tetraethylammonium chloride (TEA). *B*: representative force tracings from guinea pig tracheal rings precontracted with TEA. Spontaneous and complete relaxation was seen following treatment with 50 μM SH-053-2′F-R-CH$_3$ (*bottom*) compared with vehicle control (*top*). *C*: compiled results illustrating enhancement of spontaneous relaxation expressed as % remaining force at 30 min following treatment with 50 μM SH-053-2′F-R-CH$_3$ from a TEA-induced contraction ($^{*}P < 0.05$; n = 5/group). *D* and *E*: SH-053-2′F-R-CH$_3$ activation of α5-containing ASM GABA$_A$ receptors induces direct relaxation of substance P (Sub P)-induced contractions. Representative tracings illustrating direct relaxation of a 1 μM substance P contraction following treatment with SH-053-2′F-R-CH$_3$ (*top tracing*) compared with vehicle control (*bottom tracing*). Compiled results demonstrating enhanced spontaneous relaxation (expressed as % remaining force at 30 min following a 1 μM substance P-mediated contraction) following treatment with SH-053-2′F-R-CH$_3$ compared with treatment with vehicle control (n = 4–5/group, $^{**}P < 0.01$).

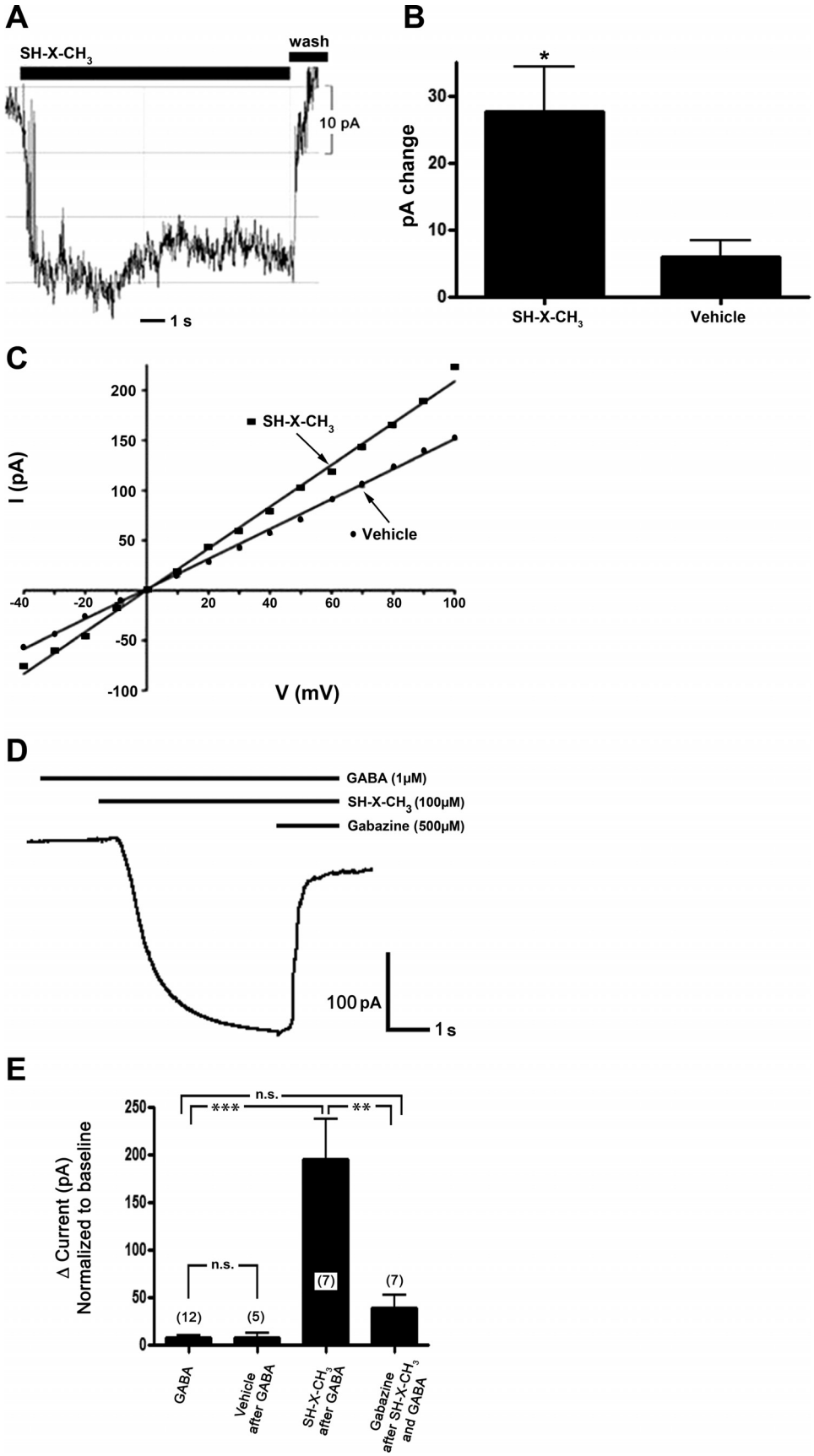

Fig. 3. Electrophysiological characterization of human ASM cells following activation of α5 containing GABA$_A$ receptors with SH-053-2′F-R-CH$_3$. *A*: representative tracing of a voltage clamp recording obtained from a single human ASM cell in whole cell configuration illustrating current evoked by application of 10 μM SH-053-2′F-R-CH$_3$ (SH-X-CH$_3$) under voltage clamp at −60 mV. *B*: compiled current changes (under voltage clamp of −60 mV) elicited in human ASM cells following application of SH-053-2′F-R-CH$_3$. Bar graph represents a −28 ± 7 pA current change after 10 μM SH-053-2′F-R-CH$_3$ treatment compared with buffer treatment demonstrating −6 ± 3 current change (n = 4/group, $^*P < 0.05$). *C*: representative current (*I*)-voltage (V) relationship obtained from voltage-clamp recordings of human ASM cells in whole cell configuration, illustrating increased chloride conductance with treatments of SH-053-2′F-R-CH$_3$ compared with buffer alone. The reversal potential obtained is consistent with a chloride current as predicted by the Nernst equation given our buffer constituents (see RESULTS). *D*: representative current tracing utilizing the Port-a-Patch single cell recording platform to illustrate GABA$_A$-specific responses. Whole cell recording of a human ASM cell illustrates current changes evoked following the sequential addition of GABA (1 μM), SH-053-2′F-R-CH$_3$ (100 μM), and then gabazine (500 μM). *E*: graph of compiled current changes evoked by GABA (1 μM), SH-053-2′F-R-CH$_3$ (100 μM) in the presence of GABA 1 μM, and gabazine 500 μM in the presence of SH-053-2′F-R-CH$_3$ (100 μM) and GABA (1 μM). Data from each cell are expressed as normalized values from stable baseline current prior to addition of any drugs (n = 5–7/group, $^{**}P < 0.01$, $^{***}P < 0.001$; n.s., not significant).

a change in the slope of the *I*-V curve with the bath application of 10 μM SH-053-2′F-R-CH$_3$ (Fig. 3*C*), indicating that chloride current in these cells was increased in the presence of SH-053-2′F-R-CH$_3$.

Automated Port-a-Patch Whole Cell Electrophysiological Recordings of Human ASM Cells also Demonstrate Current Evoked by SH-053-2′F-R-CH$_3$ Is Reversible by the Classic GABA$_A$ Channel Antagonist Gabazine

To confirm that SH-053-2′F-R-CH$_3$-mediated electrophysiological responses are GABA$_A$ receptor specific, we investigated whether currents induced by SH-053-2′F-R-CH$_3$ exposure of human ASM cells were attenuated by subsequent treatment with gabazine (Fig. 3, *D* and *E*). Compared with baseline current, we observed no significant change in current in human ASM cells upon exposure to 1 μM GABA (6 ± 2 ΔpA, $n = 5$, $P > 0.05$) or following the subsequent administration of DMSO (0.1%) vehicle (9 ± 5 ΔpA; $n = 5$, $P > 0.05$). However, we did observe a significant inward current when SH-053-2′F-R-CH$_3$ (100 μM) was applied subsequent to receiving 1 μM GABA (195 ± 44 ΔpA; $n = 7$, vs. 8 ± 5 ΔpA; $n = 7$, respectively; $P < 0.001$). We also observed a significant reversal of current when gabazine (500 μM) was subsequently applied to cells that received SH-053-2′F-R-CH$_3$ (39 ± 9 ΔpA; $n = 7$, $P < 0.01$) compared with the current generated by SH-053-2′F-R-CH$_3$ (194.8 ± 43.5 ΔpA; $n = 7$). Gabazine-induced change in current was not significantly different compared with current obtained from the preceding 1 μM GABA treatment. A representative tracing of the current induced by SH-053-2′F-R-CH$_3$ and its subsequent attenuation by a GABA$_A$-specific antagonist (gabazine) is shown in Fig. 3*D*.

SH-053-2′F-R-CH$_3$ Attenuates Contractile Agonist Mediated Rise in [Ca^{2+}]$_i$ That Is Significantly Attenuated by the GABA$_A$ Antagonist Gabazine

We next investigated the effect of SH-053-2′F-R-CH$_3$ on Ca^{2+} regulation under three paradigms: increases in bradykinin-induced $[Ca^{2+}]_i$ in the presence and absence of extracellular Ca^{2+}, and SOCE. Pretreatment with 10 μM SH-053-2′F-R-CH$_3$ significantly attenuated the increase in $[Ca^{2+}]_i$ induced by 1 μM bradykinin, and this effect of SH-053-2′F-R-CH$_3$ was eliminated if the cells were simultaneously pretreated with the GABA$_A$ antagonist gabazine (200 μM) (Fig. 4, *A* and *B*) ($n = 8$–23/group, $P < 0.01$). Gabazine pretreatment alone had no significant effect on bradykinin-induced increases in $[Ca^{2+}]_i$. These studies were then repeated under conditions of normal vs. zero external $[Ca^{2+}]$. As expected, zero external $[Ca^{2+}]$ reduced the magnitude of the bradykinin-induced increases in $[Ca^{2+}]_i$, but in the absence of extracellular Ca^{2+} SH-053-2′F-R-CH$_3$ pretreatment was without effect on bradykinin-induced $[Ca^{2+}]_i$ (Fig. 4, *C* and *D*) ($n = 6$–10/group; $P < 0.05$). These results suggest that the component of bradykinin-induced $[Ca^{2+}]_i$ increase affected by SH-053-2′F-R-CH$_3$ is occurring at the level of plasma membrane Ca^{2+} entry.

Activation of α5-Containing GABA$_A$ Receptors Inhibits Store-Operated Ca^{2+} Entry into Human ASM Cells

SOCE is an important mechanism of refilling the SR with Ca^{2+} following the emptying of the SR following activation of Gq-coupled receptors by agents such as bradykinin. SH-053-2′F-R-CH$_3$ 100 μM resulted in a significant reduction in Ca^{2+} influx upon reintroduction of external Ca^{2+} in human ASM cells previously rendered SR Ca^{2+} depleted by treatment with the SERCA inhibitor thapsigargin, signifying an inhibition of SOCE (Fig. 5, $n = 5$–8/group, $P < 0.01$). This effect of SH-053-2′F-R-CH$_3$ was reversed by simultaneous pretreatment with the GABA$_A$ receptor antagonist gabazine. SKF 96365, a known SOCE inhibitor, served as a positive control for our assay and also led to a significant decrease in Ca^{2+} influx (Fig. 5, $n = 5$–8/group, $P < 0.05$).

SH-053-2′F-R-CH$_3$ Attenuates Methacholine-Induced Peripheral Airway Contractions and Ca^{2+} Oscillations

Airway lumen area in the peripheral regions of mouse lungs decreased to ~35% of the initial resting luminal area upon stimulation with 0.3 μM methacholine (MCh) (Fig. 6*A*) ($n = 4$ airways, $P < 0.001$ compared with baseline). This airway constriction was acutely reversed when SH-053-2′F-R-CH$_3$ (100 μM) was added to the perfusing buffer in the continued presence of 0.3 μM MCh, allowing the airways to dilate to ~90% of their initial luminal area (Fig. 6*A*) ($n = 4$ airways, $P < 0.001$ comparing MCh to MCh + SH-X-053). Washing out of the SH-X-053 while maintaining 0.3 μM MCh in the perfusing buffer resulted in a reconstriction of the airway to nearly the same magnitude as the initial MCh-induced airway constriction. Finally, washout of the MCh allowed dilation of the airways back to their original resting luminal area.

We then measured Ca^{2+} oscillations induced by MCh in ASM cells of mouse lung slice while simultaneously measuring luminal area (Fig. 6*B*). MCh induced Ca^{2+} oscillations at ~14 spikes/min, and these were totally eliminated by the addition of the GABA$_A$ receptor α5 ligand SH-053-2′F-R-CH$_3$ (100 μM) (Fig. 6*B* and Supplemental Video S1; Supplemental Material for this article is available on the Journal website) ($n = 4$ airways, $P < 0.001$ comparing MCh to MCh + SH-053-2′F-R-CH$_3$). The induction of Ca^{2+} oscillations by MCh was accompanied by a reduction in airway luminal area to ~40% of the initial luminal area. This airway constriction relaxed with the addition of SH-053-2′F-R-CH$_3$ and was concomitant with the loss of Ca^{2+} oscillations.

DISCUSSION

The major findings of this study are that human ASM possesses GABA$_A$ receptors with an α5-subunit profile that can be pharmacologically targeted by a selective ligand. In intact human ASM the GABA$_A$ receptor α5-subunit-selective ligand (SH-053-2′F-R-CH$_3$) enhanced β-adrenoceptor agonist-mediated relaxation. In intact guinea pig ASM the GABA$_A$ receptor α5-subunit-selective ligand relaxes an established contraction induced by membrane depolarization (TEA) or by activation of a Gq-coupled neurokinin receptor. In isolated human ASM cells this GABA$_A$ receptor α5-subunit-targeting ligand elicits a Cl^- current, consistent with GABA$_A$ receptor activation, and attenuates multiple mechanisms of plasma membrane Ca^{2+} entry.

The expression of only two subtypes of GABA$_A$ receptor α-subunits in human ASM (only α4 and α5 are expressed) is an important consideration since these subunits play a key role in determining GABA$_A$ receptor localization and pharmacology (20, 37). The α-subunit plays a critical role in ligand (both

agonist and allosteric) binding. This is illustrated by the binding of classical 1,4 benzodiazepines at the interface of γ- and α-subunits of α1-, α2-, α3-, and α5-subunit-containing GABA$_A$ receptors (43) but not at GABA$_A$ receptors containing α4- or α6-subunits (12, 47). Furthermore, among the active benzodiazepine α-subunits (α1, α2, α3, or α5), there are differential pharmacological profiles such that different α-subunits confer varied drug affinities. This has been shown for the nonclassical benzodiazepine agonist zolpidem, which demonstrates highest affinity for receptors containing the α1-subunit, followed by receptors containing an α2- or α3-subunit (35), and α5-subunit-containing receptors displaying an exceedingly low affinity (2, 38). These studies laid the foundation for subsequent studies that have established that particular drug effects associated with classical benzodiazepine agonists (se-

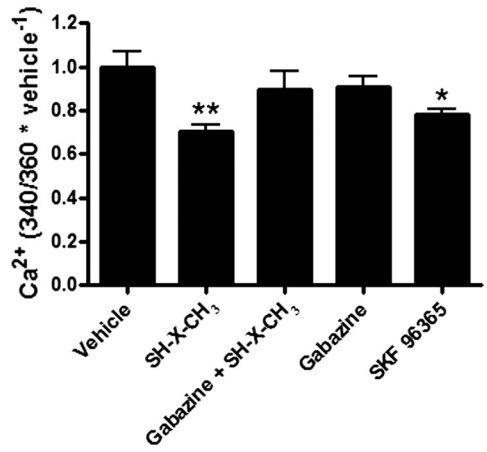

Fig. 5. The GABA$_A$ receptor α5-subunit-targeting ligand SH-053-2′F-R-CH$_3$ inhibits store-operated Ca^{2+} reentry. Immortalized human ASM cells incubated in zero $[Ca^{2+}]_i$ solution and treated with thapsigargin (1 μM) allowed for depletion of SR Ca^{2+} stores. Ca^{2+} (2.5 mM) was then added to the external buffer and the resulting $[Ca^{2+}]_i$ peaks (assayed by Fura-2 AM 340/380 emission) are presented as fraction of the effect of vehicle alone. SH-053-2′F-R-CH$_3$ (SH-X-CH$_3$) (100 μM) and known store-operated Ca^{2+} entry (SOCE) inhibitor SKF 96365 (10 μM) significantly inhibited SOCE. The effect of SH-053-2′F-R-CH$_3$ was completely reversed with GABA$_A$ receptor antagonist gabazine (100 μM) (n = 5–8/group. *P < 0.05; **P < 0.01).

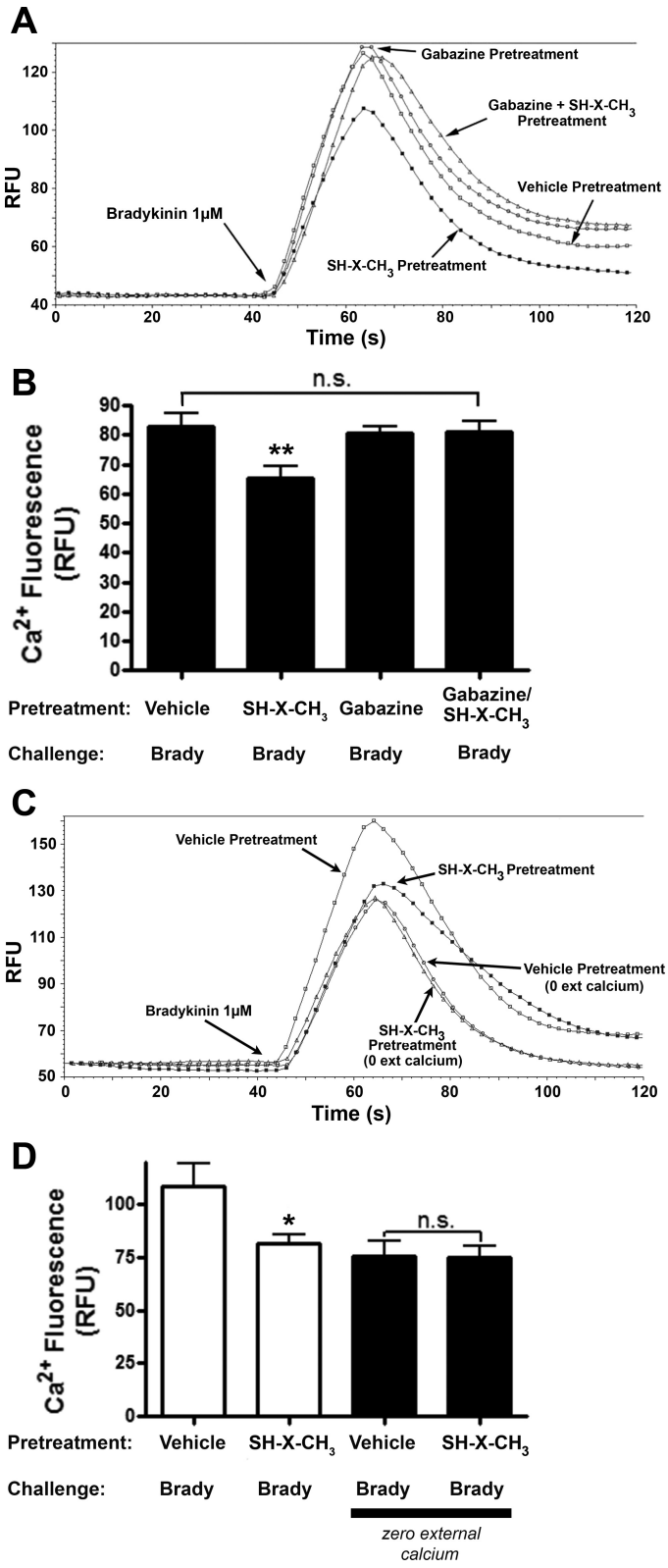

Fig. 4. Activation of α5-containing GABA$_A$ receptors inhibits cellular Ca^{2+} handling. *A* and *B*: the GABA$_A$ α5-subunit-targeting ligand SH-053-2′F-R-CH$_3$ attenuates bradykinin (Brady)-induced intracellular Ca^{2+} concentration ($[Ca^{2+}]_i$) increase. *A*: representative tracing of Fluo-4 fluorescence (RFU) from cultured human ASM cells pretreated for 15 min with either SH-053-2′F-R-CH$_3$ (SH-X-CH$_3$) (10 μM), gabazine (200 μM), gabazine (200 μM) and SH-053-2′F-R-CH$_3$ (10 μM), or vehicle control (0.1% DMSO) followed by treatment with bradykinin (1 μM). *B*: SH-053-2′F-R-CH$_3$ attenuates bradykinin-induced $[Ca^{2+}]_i$ increase (65 ± 4 RFU; n = 21) compared with vehicle control (83 ± 4 RFU; n = 23; **P < 0.01). Blocking the GABA$_A$ receptor with the antagonist gabazine has no significant effect on bradykinin-induced $[Ca^{2+}]_i$ increase (81 ± 2 RFU; n = 8) compared with vehicle control. Moreover, the ability of SH-053-2′F-R-CH$_3$ to attenuate bradykinin-induced $[Ca^{2+}]_i$ increase is prevented in cells first pretreated with gabazine (Gabazine + SH-053-2′F-R-CH$_3$: 81 ± 3 RFU; n = 23), illustrating that this is a GABA$_A$ receptor mediated effect of the ligands. *C* and *D*: SH-053-2′F-R-CH$_3$ attenuation of bradykinin-induced intracellular Ca^{2+} increase requires extracellular Ca^{2+}. *C*: representative tracing of Fluo-4 fluorescence (RFU) from cultured human ASM cells pretreated for 15 min with either SH-053-2′F-R-CH$_3$ (10 μM) or vehicle (0.1% DMSO), in the presence or absence of external (ext) Ca^{2+}, followed by treatment with bradykinin (1 μM). *D*: compiled results illustrating SH-053-2′F-R-CH$_3$ attenuates bradykinin-induced $[Ca^{2+}]_i$ increase (82 ± 5 RFU; n = 8) compared with vehicle control (109 ± 11 RFU; n = 6; *P < 0.05). However, in the absence of extracellular Ca^{2+}, SH-053-2′F-R-CH$_3$ does not significantly attenuate bradykinin-induced $[Ca^{2+}]_i$ increase (75 ± 5 RFU; n = 10) compared with vehicle control (76 ± 7 RFU; n = 10), suggesting that SH-053-2′F-R-CH$_3$'s effect is on a component of external Ca^{2+} entry.

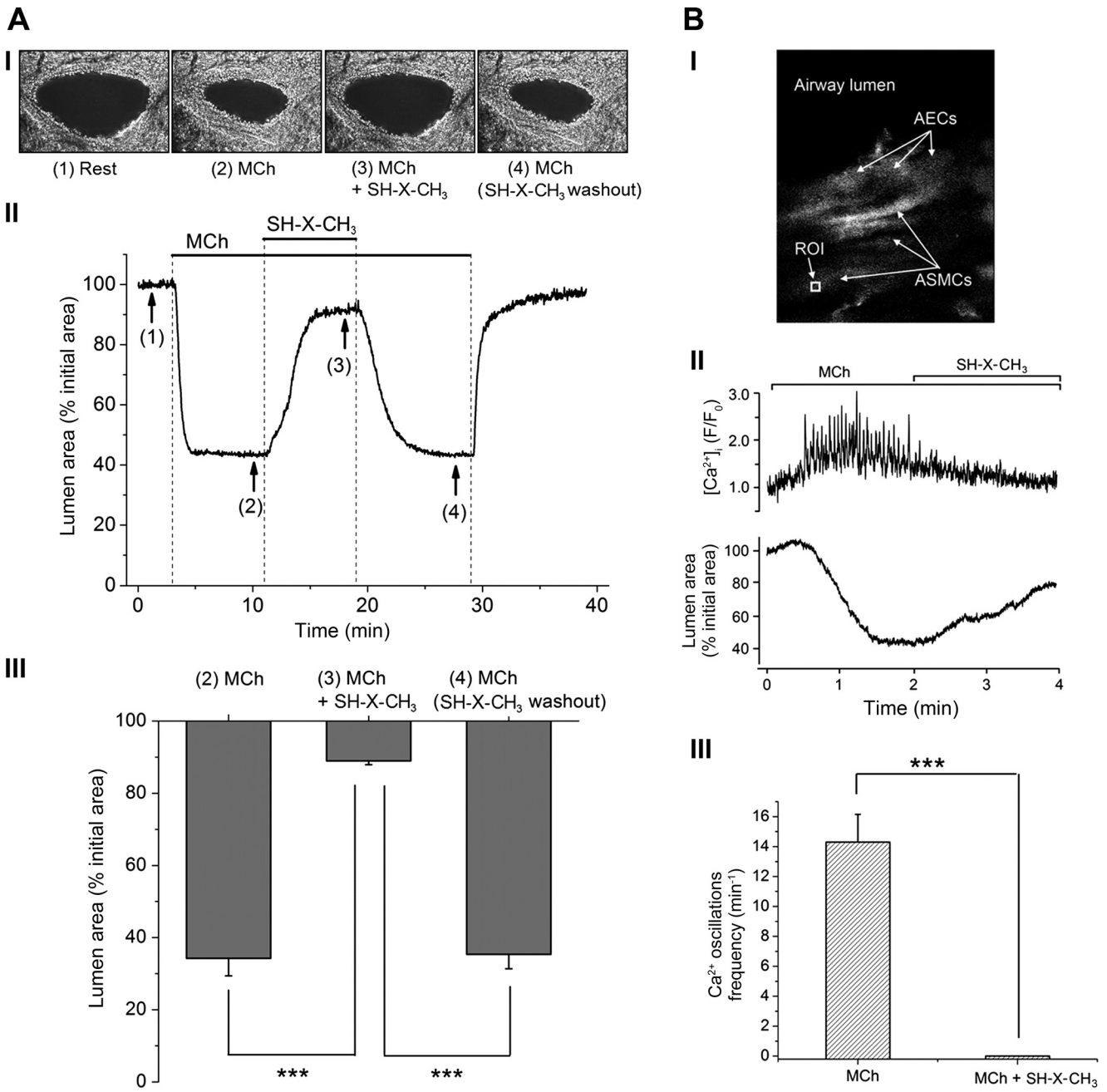

Fig. 6. *A*: SH-053-2′F-R-CH$_3$ relaxes small peripheral murine airway slices precontracted with methacholine (MCh). Contractile response of mouse small airways to MCh and relaxation induced by GABA$_A$ α5-subunit selective ligand SH-053-2′F-R-CH$_3$ (SH-X-CH$_3$). *I*: representative phase-contrast images showing a small airway in a lung slice before stimulation (1), after stimulation with 0.3 μM MCh (2), after the addition of 100 μM SH-X-CH$_3$ in the continued presence of MCh (3), and after washout of SH-X-CH$_3$ in the continued presence of MCh (4), taken at the times indicated by arrows and corresponding to the numbers in the trace shown in *II*. *II*: representative tracing of changes in airway lumen cross-sectional area during superfusion with MCh with the addition and washout of SH-X-CH$_3$ (upper lines). Washout of stimuli was performed by superfusion of lung slices with HBSS. *III*: summary of sustained airway contraction measured as the decrease in lumen area after the addition of MCh or SH-X-CH$_3$ at the times indicated in *B*. Data are means ± SE of 4 airways (each from a different lung slice) from 2 mice. ***$P < 0.001$ compared with MCh + SH-X-CH$_3$. *B*: SH-053-2′F-R-CH$_3$ abolishes MCh induced calcium oscillations in peripheral murine airway slices. Simultaneous Ca^{2+} signaling and contraction in ASM cells induced by MCh and reversed by the GABA$_A$ receptor α5-subunit selective ligand SH-X-CH$_3$. *I*: fluorescence confocal image of an airway region in a lung slice showing epithelial cells (AECs) lining the airway lumen (*top left*, black area) and the underlying ASM cells (ASMCs). A small (7 × 7-pixel) region of interest (ROI) within an ASM cell indicate the areas selected for the representative fluorescence trace presented in *II*. *II*: fluorescence (F/F_0) trace showing the Ca^{2+} oscillations stimulated by 0.3 μM MCh and then inhibited by 100 μM SH-X-CH$_3$ in a single ASM cell while measuring airway lumen area. *III*: compiled graph of data is representative of 4 experiments in lung slices from 2 mice (***$P < 0.001$). A time-lapse movie showing the Ca^{2+} oscillations stimulated by MCh and inhibited by SH-X-CH$_3$ is shown in Supplemental Video S1.

dation, anxiolysis, ataxia, and amnesia) are α-subunit dependent. More specifically, GABA$_A$ receptors containing α1-subunits are thought to be primarily responsible for the sedative effects of benzodiazepines, whereas α2- and α3-subunits are implicated in the anxiolytic effects of benzodiazepines (13, 30, 32, 40). Finally, GABA$_A$ receptors containing α5-subunits are a relatively minor population in the CNS that may play a role in memory processes, but not in motor or sedation effects (9). This underlies a secondary potential benefit of drugs targeting α5-subunit-containing GABA$_A$ receptors, namely that they are devoid of many potentially negative CNS side effects.

As mentioned earlier, pharmacophore receptor models for the α1–6β3γ2 benzodiazepine/GABA$_A$-ergic subtypes were developed in the 1980s and refined in the 1990s. This led to the synthesis of a series of chiral R- and S-isomers of earlier imidazobenzodiazepines that exhibited subtype selectivity at α2 and α3 subtypes. However, as reported in Fischer et al. (14), the in vitro binding affinity of SH-053-2′F-R-CH$_3$ was clearly higher at α5β3γ2 subtypes with very little affinity at α1, α2, or α3 subtypes [K_i values: α1β3γ2 (759.1), α2 (948.2), α3 (768.8), and α5 (95.2) nM]. The C-6 pendent phenyl ring of SH-053-2′F-R-CH$_3$ is incompatible with binding at α4 and α6 diazepam-insensitive benzodiazepine GABA receptors. Moreover, the efficacy in oocytes (% control currents) at α5-subtypes was higher than at the other three subtypes (14). In addition, the in vivo data for SH-053-2′F-R-CH$_3$ compared with diazepam in primates clearly show that SH-053-2′F-R-CH$_3$ is not sedating (α1 activity is low) and that the anxiolytic activity of this R-CH$_3$ isomer is either very weak or nonexistent. This indicates that this R-CH$_3$ isomer does not activate α2 or α3 BDZ receptor subtypes to any appreciable extent in this primate conflict model.

With the targeted development of allosteric GABA$_A$ receptor ligands with selectivity for GABA$_A$ receptors containing α5-subunits, it is particularly fortuitous that the repertoire of GABA$_A$ receptor α-subunits on human ASM is restricted to only the α4- and α5-subunits. Indeed, we have previously shown that a ligand selective for the α4-subunit (CMD-45) as well as gaboxadol, a well-known ligand with α4 selectivity, regulate ASM tone (18). Thus a goal of the present study was to determine whether α5 targeting could also realize these beneficial effects of ASM contractile tone. We also sought to determine whether $[Ca^{2+}]_i$, a critical regulator of ASM tone, was regulated by GABA$_A$ receptor α5-subunit-targeting ligands.

One component of asthma is the enhanced mass and contraction of ASM and drugs used for the acute relief of an asthmatic exacerbation target acute relaxation of ASM. The leading pharmaceutical drug class for this critical clinical therapy is β-adrenoceptor agonists, and in the present study we demonstrate that SH-053-2′F-R-CH$_3$ augmented the relaxation effect of a β-agonist in intact human ASM. These findings suggest a clinically relevant role for targeting α5-subunit-containing GABA$_A$ receptors in the acute relaxation of human ASM.

We next demonstrated that SH-053-2′F-R-CH$_3$ alone could relax an established contraction by a depolarizing stimulus (TEA) or a G$_q$-coupled ligand (substance P) in guinea pig ASM. These results also highlight an important mechanistic fact regarding SH-053-2′F-R-CH$_3$ mediated relaxation, namely that GABA$_A$ receptor mediated-relaxation does not involve K^+ channels. So, whereas β-adrenoceptor relaxation does involve a component of PKA-mediated large conductance K_{Ca} channel activation (and SH-053-2′F-R-CH$_3$ mediated GABA$_A$ activation does augment isoproterenol relaxation), SH-053-2′F-R-CH$_3$'s capacity to relax a TEA contraction (achieved by K^+ channel blockade) suggests complementary mechanisms of relaxation, not mechanistic overlap at the same receptor or K^+ channel. The relaxation of SH-053-2′F-R-CH$_3$ in these ex vivo muscle force studies in human and guinea pig ASM under several different contraction/relaxation paradigms led us to investigate accompanying cellular events in cultured human ASM cells.

Whole cell electrophysiology experiments demonstrated a current with a reversal potential at the predicted voltage for chloride, and this chloride current was enhanced in the presence of SH-053-2′F-R-CH$_3$ and blocked by the GABA$_A$ receptor antagonist gabazine. A chloride current at the plasma membrane would change membrane potential of the plasma membrane, which in turn may modulate numerous Ca^{2+} entry pathways. Although Ca^{2+} control in an ASM cell is complex, involving multiple channels, exchangers, and pumps on both the plasma membrane and intracellular organelles, a component of intracellular Ca^{2+} handling is regulated by membrane potential. Indeed, in addition to voltage-gated Ca^{2+} channels (19), Na^+/Ca^{2+} exchangers (22, 31), nonselective cation channels of the TRP family (7), and perhaps even SOCE are all influenced by membrane potential (29).

$[Ca^{2+}]_i$ was measured before and after the addition of the Gq-coupled receptor agonist bradykinin in the presence and absence of extracellular Ca^{2+}. As expected, in the absence of extracellular Ca^{2+}, the bradykinin-induced levels of $[Ca^{2+}]_i$ were ~80% of the Ca^{2+} levels achieved in the presence of extracellular Ca^{2+}, consistent with the dogma that Gq-coupled ligands' primary source of Ca^{2+} is from intracellular stores. Interestingly, in the presence of extracellular Ca^{2+}, SH-053-2′F-R-CH$_3$ reduced bradykinin-induced $[Ca^{2+}]_i$ by ~20%, which likely represents the total amount of extracellular Ca^{2+} influx during bradykinin treatment. This was supported by additional experiments in which SH-053-2′F-R-CH$_3$ was without effect in the absence of extracellular Ca^{2+}. These findings suggest that SH-053-2′F-R-CH$_3$ is blocking the component of bradykinin-induced $[Ca^{2+}]_i$ that arises from extracellular sources, which is likely a complex acute response involving Ca^{2+} exchangers and SOCE to refill the cytosol and SR. To further investigate whether SH-053-2′F-R-CH$_3$ also modulates Ca^{2+} handling relevant to the maintenance phase of a contraction, we performed additional studies examining the role of SH-053-2′F-R-CH$_3$-mediated GABA$_A$ activation on SOCE and calcium oscillations in airway slices.

Following the release of SR Ca^{2+} in ASM, an influx of extracellular Ca^{2+} occurs to refill the SR store, a process referred to as SOCE (27). SH-053-2′F-R-CH$_3$ led to a significant decrease in SOCE via a GABA$_A$ receptor-specific effect since it is reversed by the GABA$_A$ receptor antagonist gabazine.

In ASM, the resting membrane potential is thought to be approximately −60 mV and the reversal potential of chloride is thought to be approximately −20 to −30 mV (28). Thus GABA$_A$ agonists would lead to a depolarization of ASM resting membrane potential. In lymphocytes, a cell type in

which SR store-operated Ca^{2+} influx has been extensively studied owing to its key role in T cell receptor-mediated cellular activation and proliferation, membrane depolarization is known to greatly inhibit store-operated Ca^{2+} influx, likely by reducing the driving force for Ca^{2+} entry through the STIM-ORAI complex (3, 24). Since $GABA_A$ activation is predicted to depolarize ASM resting membrane potential, a similar effect may be occurring in this in vitro SOCE assay with ASM.

However, in contrast to effects at membrane potential-contracted ASM, after Gq-coupled receptor activation for example, the membrane potential is expected to be depolarized. Under these conditions, $GABA_A$ activation would be expected to lead to a relative hyperpolarization, which would increase the electrostatic driving force for extracellular Ca^{2+} entry. This would seem at odds with the ability of $GABA_A$ agonists to relax precontracted ASM in organ bath preparations. However, under these conditions, this relative hyperpolarization may inhibit capacitive Ca^{2+} influx via voltage sensitive L-type Ca^{2+} channels and/or the reverse mode of the Ca^{2+}-sodium exchanger, which have been shown to be key in ASM for maintaining intracellular Ca^{2+} necessary to sustain contraction (22). Further studies are needed to confirm this hypothesis.

In contrast to the findings presented in the current study with an allosteric agonist of the $GABA_A$ chloride channel, our laboratory has also demonstrated that antagonists of another family of chloride channels (calcium-activated chloride channels, TMEM16, or anoctamin) can also mediate ASM relaxation (11, 16, 45). It may appear surprising that agonism of one type of chloride channel could result in the same physiological effect as antagonism of a different family of chloride channels. These interesting findings were addressed in an editorial focus by Dr. Janssen (26) that presented a number of mechanistic hypotheses to account for seemingly opposing effects of ligand-gated $GABA_A$ channels vs. calcium- and voltage-gated calcium-activated chloride channels. These mechanistic differences include an oscillating membrane potential from electrical slow waves, distribution of different types of chloride channels on the plasma membrane vs. intracellular organelles, cytosolic compartmentalization of chloride (as is already known to exist for calcium), and the possibility that intracellular effectors can interact with certain ion channels (or whether chloride itself acts) in certain microdomains to modulate other intracellular contractile effectors. These spatial and temporal mechanisms may be quite different in calcium-activated chloride channels, which are regulated by both calcium and voltage (4), compared with $GABA_A$ chloride channels, which are ligand gated.

In summary, we present the following evidence: *1*) that targeting of α5 $GABA_A$ α-subunits in ASM produces characteristic electrophysiological changes indicative of $GABA_A$ receptor activation, *2*) that this selective agonist can augment β-agonist-mediated relaxation, *3*) that $GABA_A$ α5 receptor activation can directly and spontaneously relax precontracted ASM, and *4*) that a component of the mechanism involves an attenuation of Ca^{2+} handling (as reductions in both agonist-induced external Ca^{2+} entry and reductions in SOCE in human ASM cells as well as in calcium oscillations in ASM within intact peripheral lung slices). As such, these studies hold promise and potential for improving the armamentarium of pharmacological agents available to treat acute airway bronchoconstriction and suggest a novel role for chloride in the modulation of Ca^{2+} handing in ASM.

GRANTS

This work was supported by National Institutes of Health Grants GM065281 (C. W. Emala), GM008464 (C. W. Emala), HL118561 (J. M. Cook), and GM093137 (G. Gallos).

DISCLOSURES

No conflicts of interest, financial or otherwise, are declared by the author(s).

AUTHOR CONTRIBUTIONS

G.G., G.T.Y., J.M.C., N.H., J.F.P.-Z., and C.W.E. conception and design of research; G.G., G.T.Y., M.E.S., P.D.Y., X.W.F., M.M.P., and J.F.P.-Z. performed experiments; G.G., G.T.Y., M.E.S., P.D.Y., X.W.F., and J.F.P.-Z. analyzed data; G.G., P.D.Y., and C.W.E. interpreted results of experiments; G.G., G.T.Y., M.E.S., P.D.Y., X.W.F., and J.F.P.-Z. prepared figures; G.G. and C.W.E. drafted manuscript; G.G., G.T.Y., M.M.P., J.M.C., N.H., J.F.P.-Z., and C.W.E. edited and revised manuscript; G.G., G.T.Y., M.E.S., P.D.Y., X.W.F., M.M.P., J.M.C., N.H., J.F.P.-Z., and C.W.E. approved final version of manuscript.

REFERENCES

1. **az-Arauzo H, Koehler KF, Hagen TJ, Cook JM.** Synthetic and computer assisted analysis of the pharmacophore for agonists at benzodiazepine receptors. *Life Sci* 49: 207–216, 1991.
2. **Burgard EC, Tietz EI, Neelands TR, Macdonald RL.** Properties of recombinant gamma-aminobutyric acid A receptor isoforms containing the alpha 5 subunit subtype. *Mol Pharmacol* 50: 119–127, 1996.
3. **Cahalan MD, Chandy KG.** The functional network of ion channels in T lymphocytes. *Immunol Rev* 231: 59–87, 2009.
4. **Caputo A, Caci E, Ferrera L, Pedemonte N, Barsanti C, Sondo E, Pfeffer U, Ravazzolo R, Zegarra-Moran O, Galietta LJ.** TMEM16A, a membrane protein associated with calcium-dependent chloride channel activity. *Science* 322: 590–594, 2008.
5. **Castro-Piedras I, Perez-Zoghbi JF.** Hydrogen sulphide inhibits Ca^{2+} release through InsP3 receptors and relaxes airway smooth muscle. *J Physiol* 591: 5999–6015, 2013.
6. **Chu EK, Drazen JM.** Asthma: one hundred years of treatment and onward. *Am J Respir Crit Care Med* 171: 1202–1208, 2005.
7. **Clapham DE.** TRP channels as cellular sensors. *Nature* 426: 517–524, 2003.
8. **Clayton T, Chen JL, Ernst M, Richter L, Cromer BA, Morton CJ, Ng H, Kaczorowski CC, Helmstetter FJ, Furtmuller R, Ecker G, Parker MW, Sieghart W, Cook JM.** An updated unified pharmacophore model of the benzodiazepine binding site on gamma-aminobutyric acid(a) receptors: correlation with comparative models. *Curr Med Chem* 14: 2755–2775, 2007.
9. **Collinson N, Kuenzi FM, Jarolimek W, Maubach KA, Cothliff R, Sur C, Smith A, Otu FM, Howell O, Atack JR, McKernan RM, Seabrook GR, Dawson GR, Whiting PJ, Rosahl TW.** Enhanced learning and memory and altered GABAergic synaptic transmission in mice lacking the alpha 5 subunit of the $GABA_A$ receptor. *J Neurosci* 22: 5572–5580, 2002.
10. **Cook CD, Mead J, Schreiner GL, Frank NR, Craig JM.** Pulmonary mechanics during induced pulmonary edema in anesthetized dogs. *J Appl Physiol* 14: 177–186, 1959.
11. **Danielsson J, Yim P, Rinderspacher A, Fu XW, Zhang Y, Landry DW, Emala CW.** Chloride channel blockade relaxes airway smooth muscle and potentiates relaxation by β-agonists. *Am J Physiol Lung Cell Mol Physiol* 307: L273–L282, 2014.
12. **Derry JM, Dunn SM, Davies M.** Identification of a residue in the gamma-aminobutyric acid type A receptor alpha subunit that differentially affects diazepam-sensitive and -insensitive benzodiazepine site binding. *J Neurochem* 88: 1431–1438, 2004.
13. **Dixon CI, Rosahl TW, Stephens DN.** Targeted deletion of the GABRA2 gene encoding alpha2-subunits of GABA(A) receptors facilitates performance of a conditioned emotional response, and abolishes anxiolytic effects of benzodiazepines and barbiturates. *Pharmacol Biochem Behav* 90: 1–8, 2008.
14. **Fischer BD, Licata SC, Edwankar RV, Wang ZJ, Huang S, He X, Yu J, Zhou H, Johnson EM Jr, Cook JM, Furtmuller R, Ramerstorfer J,**

Sieghart W, Roth BL, Majumder S, Rowlett JK. Anxiolytic-like effects of 8-acetylene imidazobenzodiazepines in a rhesus monkey conflict procedure. *Neuropharmacology* 59: 612–618, 2010.
15. **Gallos G, Gleason NR, Zhang Y, Pak SW, Sonett JR, Yang J, Emala CW.** Activation of endogenous GABA$_A$ channels on airway smooth muscle potentiates isoproterenol mediated relaxation. *Am J Physiol Lung Cell Mol Physiol* 295: L1040–L1047, 2008.
16. **Gallos G, Remy KE, Danielsson J, Funayama H, Fu XW, Chang HY, Yim PD, Xu D, Emala CW Sr.** Functional expression of the TMEM16 family of calcium activated chloride channels in airway smooth muscle. *Am J Physiol Lung Cell Mol Physiol* 305: L625–L634, 2013.
17. **Gallos G, Townsend EA, Yim P, Virag L, Zhang Y, Xu D, Bacchetta M, Emala CW.** Airway epithelium is a predominant source of endogenous airway GABA and contributes to relaxation of airway smooth muscle tone. *Am J Physiol Lung Cell Mol Physiol* 304: L191–L197, 2013.
18. **Gallos G, Yim P, Chang S, Zhang Y, Xu D, Cook JM, Gerthoffer WT, Emala CW Sr.** Targeting the restricted α-subunit repertoire of airway smooth muscle GABA$_A$ receptors augments airway smooth muscle relaxation. *Am J Physiol Lung Cell Mol Physiol* 302: L248–L256, 2012.
19. **Gosens R, Stelmack GL, Dueck G, McNeill KD, Yamasaki A, Gerthoffer WT, Unruh H, Gounni AS, Zaagsma J, Halayko AJ.** Role of caveolin-1 in p42/p44 MAP kinase activation and proliferation of human airway smooth muscle. *Am J Physiol Lung Cell Mol Physiol* 291: L523–L534, 2006.
20. **Hevers W, Luddens H.** The diversity of GABA$_A$ receptors. Pharmacological and electrophysiological properties of GABA$_A$ channel subtypes. *Mol Neurobiol* 18: 35–86, 1998.
21. **Hirota S, Helli P, Janssen LJ.** Ionic mechanisms and Ca^{2+} handling in airway smooth muscle. *Eur Respir J* 30: 114–133, 2007.
22. **Hirota S, Janssen LJ.** Store-refilling involves both L-type calcium channels and reverse-mode sodium-calcium exchange in airway smooth muscle. *Eur Respir J* 30: 269–278, 2007.
23. **Hirota S, Trimble N, Pertens E, Janssen LJ.** Intracellular Cl^- fluxes play a novel role in Ca^{2+} handling in airway smooth muscle. *Am J Physiol Lung Cell Mol Physiol* 290: L1146–L1153, 2006.
24. **Hogan PG, Lewis RS, Rao A.** Molecular basis of calcium signaling in lymphocytes: STIM and ORAI. *Annu Rev Immunol* 28: 491–533, 2010.
25. **Huang Q, He X, Ma C, Liu R, Yu S, Dayer CA, Wenger GR, McKernan R, Cook JM.** Pharmacophore/receptor models for GABA(A)/BzR subtypes (alpha1beta3gamma2, alpha5beta3gamma2, and alpha6beta3gamma2) via a comprehensive ligand-mapping approach. *J Med Chem* 43: 71–95, 2000.
26. **Janssen LJ.** Airway smooth muscle electrophysiology in a state of flux? *Am J Physiol Lung Cell Mol Physiol* 302: L730–L732, 2012.
27. **Janssen LJ, Kwan CY.** ROCs and SOCs: what's in a name? *Cell Calcium* 41: 245–247, 2007.
28. **Janssen LJ, Sims SM.** Ca^{2+}-dependent Cl^- current in canine tracheal smooth muscle cells. *Am J Physiol Cell Physiol* 269: C163–C169, 1995.
29. **Lewis RS, Cahalan MD.** Potassium and calcium channels in lymphocytes. *Annu Rev Immunol* 13: 623–653, 1995.
30. **Low K, Crestani F, Keist R, Benke D, Brunig I, Benson JA, Fritschy JM, Rulicke T, Bluethmann H, Mohler H, Rudolph U.** Molecular and neuronal substrate for the selective attenuation of anxiety. *Science* 290: 131–134, 2000.
31. **McCarron JG, Walsh JV Jr, Fay FS.** Sodium/calcium exchange regulates cytoplasmic calcium in smooth muscle. *Pflügers Arch* 426: 199–205, 1994.
32. **McKernan RM, Rosahl TW, Reynolds DS, Sur C, Wafford KA, Atack JR, Farrar S, Myers J, Cook G, Ferris P, Garrett L, Bristow L, Marshall G, Macaulay A, Brown N, Howell O, Moore KW, Carling RW, Street LJ, Castro JL, Ragan CI, Dawson GR, Whiting PJ.** Sedative but not anxiolytic properties of benzodiazepines are mediated by the GABA(A) receptor alpha1 subtype. *Nat Neurosci* 3: 587–592, 2000.
33. **Mizuta K, Xu D, Pan Y, Comas G, Sonett JR, Zhang Y, Panettieri RA Jr, Yang J, Emala CW Sr.** GABA$_A$ receptors are expressed and facilitate relaxation in airway smooth muscle. *Am J Physiol Lung Cell Mol Physiol* 294: L1206–L1216, 2008.
34. **Mukherjee S, Trice J, Shinde P, Willis RE, Pressley TA, Perez-Zoghbi JF.** Ca^{2+} oscillations, Ca^{2+} sensitization, and contraction activated by protein kinase C in small airway smooth muscle. *J Gen Physiol* 141: 165–178, 2013.
35. **Munakata M, Jin YH, Akaike N, Nielsen M.** Temperature-dependent effect of zolpidem on the GABA$_A$ receptor-mediated response at recombinant human GABA$_A$ receptor subtypes. *Brain Res* 807: 199–202, 1998.
36. **O'Byrne PM, Reddel HK, Eriksson G, Ostlund O, Peterson S, Sears MR, Jenkins C, Humbert M, Buhl R, Harrison TW, Quirce S, Bateman ED.** Measuring asthma control: a comparison of three classification systems. *Eur Respir J* 36: 269–276, 2010.
37. **Olsen RW, Sieghart W.** GABA A receptors: subtypes provide diversity of function and pharmacology. *Neuropharmacology* 56: 141–148, 2009.
38. **Puia G, Vicini S, Seeburg PH, Costa E.** Influence of recombinant gamma-aminobutyric acid-A receptor subunit composition on the action of allosteric modulators of gamma-aminobutyric acid-gated Cl^- currents. *Mol Pharmacol* 39: 691–696, 1991.
39. **Rahman M, Inman M, Kiss L, Janssen LJ.** Reverse-mode NCX current in mouse airway smooth muscle: Na^+ and voltage dependence, contributions to Ca^{2+} influx and contraction, and altered expression in a model of allergen-induced hyperresponsiveness. *Acta Physiol (Oxf)* 205: 279–291, 2012.
40. **Rowlett JK, Platt DM, Lelas S, Atack JR, Dawson GR.** Different GABA$_A$ receptor subtypes mediate the anxiolytic, abuse-related, and motor effects of benzodiazepine-like drugs in primates. *Proc Natl Acad Sci USA* 102: 915–920, 2005.
41. **Savic MM, Clayton T, Furtmuller R, Gavrilovic I, Samardzic J, Savic S, Huck S, Sieghart W, Cook JM.** PWZ-029, a compound with moderate inverse agonist functional selectivity at GABA(A) receptors containing alpha5 subunits, improves passive, but not active, avoidance learning in rats. *Brain Res* 1208: 150–159, 2008.
42. **Savic MM, Huang S, Furtmuller R, Clayton T, Huck S, Obradovic DI, Ugresic ND, Sieghart W, Bokonjic DR, Cook JM.** Are GABA$_A$ receptors containing alpha5 subunits contributing to the sedative properties of benzodiazepine site agonists? *Neuropsychopharmacology* 33: 332–339, 2008.
43. **Sigel E.** Mapping of the benzodiazepine recognition site on GABA(A) receptors. *Curr Top Med Chem* 2: 833–839, 2002.
44. **Townsend EA, Thompson MA, Pabelick CM, Prakash YS.** Rapid effects of estrogen on intracellular Ca^{2+} regulation in human airway smooth muscle. *Am J Physiol Lung Cell Mol Physiol* 298: L521–L530, 2010.
45. **Yim PD, Gallos G, Perez-Zhogbi JF, Trice J, Zhang Y, Siviski M, Sonett J, Emala CW.** Chloride channel blockers promote relaxation of TEA-induced contraction in airway smooth muscle. *J Smooth Muscle Res* 49: 112–124, 2013.
46. **Yim PD, Gallos G, Xu D, Zhang Y, Emala CW.** Novel expression of a functional glycine receptor chloride channel that attenuates contraction in airway smooth muscle. *FASEB J* 25: 1706–1717, 2011.
47. **Ymer S, Draguhn A, Wisden W, Werner P, Keinanen K, Schofield PR, Sprengel R, Pritchett DB, Seeburg PH.** Structural and functional characterization of the gamma 1 subunit of GABA$_A$/benzodiazepine receptors. *EMBO J* 9: 3261–3267, 1990.